PSFC/JA-05-28

The Coaxial Multipactor Experiment (CMX): A facility for investigating multipactor discharges

T. P. Graves, B. LaBombard, S. J. Wukitch,
and I.H. Hutchinson

31 October 2005

Plasma Science and Fusion Center
Massachusetts Institute of Technology
Cambridge, MA 02139 USA

This work was supported by the U.S. Department of Energy, Cooperative Grant No. DE-FC02-99ER12345. Reproduction, translation, publication, use and disposal, in whole or in part, by or for the United States government is permitted.

Submitted for publication to *Review of Scientific Instruments*..

The Coaxial Multipactor Experiment (CMX): A facility for investigating multipactor discharges

T. P. Graves,* B. LaBombard, S. Wukitch, and I. Hutchinson

Plasma Science and Fusion Center,

Massachusetts Institute of Technology, Cambridge, MA, 02139

(Dated: October 14, 2005)

Abstract

A multipactor discharge is a resonant condition for electrons in an alternating electric field. This discharge can be disruptive to radio frequency (RF) circuits, cavities, and resonators. The Coaxial Multipactor Experiment (CMX) investigates these discharges in parallel plate and coaxial transmission line geometries at frequencies from 40 to 150 MHz with goals of measuring the electron energy distributions. CMX has a unique experimental setup which allows the transmission line to pass continuously through a short vacuum region. Retarding potential analyzers with secondary electron suppression measure the electron current as a function of bias voltage. Both parallel plate and coaxial multipactor experiments provide the first detailed measurements of the electron energy distributions under a variety of RF frequencies and electrode materials.

PACS numbers: 52.80.Pi High-frequency and RF discharges

*Electronic address: tgraves@mit.edu

I. INTRODUCTION

A multipactor discharge is a low voltage phenomenon in which electrons impact one or more material surfaces in resonance with an alternating electric field [1, 2, 3]. Two main conditions must be met in order to develop a multipactor discharge between two surfaces. First, electrons traversing the gap must impact the electrode near the time the field reverses direction. Second, electrons must impact the surface with enough energy to create electron multiplication by secondary emission; i.e. $\delta(E) \geq 1$. Because the discharge is sustained by secondary electrons, multipactor discharges typically occur under vacuum conditions.

RF devices in fusion, accelerator, and space research often operate under vacuum conditions with frequencies and geometries which are susceptible to multipactoring. Multipactor discharges are generally unfavorable in these experiments because the multipactor creates a reactive component in the rf circuit which detunes the cavity and limits the circulating power. The multipactor can also dissipate rf power to the electrodes that can cause surface heating, gas desorption, or physical damage [3]. In some situations, a multipactor can induce a glow discharge at a pressure below that expected for Paschen breakdown [4].

In the frequency range of 30-300 MHz (Very High Frequency [VHF]), coaxial and stripline transmission lines are often used in rf power systems. Multipactor discharges in the linear electric field of stripline transmission lines have been studied extensively [2, 4, 5], yet little research has been done on coaxial multipactor discharges. The electric field of a coaxial transmission line is inversely proportional to the radius, and a multipactor discharge can occur in the non-uniform field. The multipactor can occur on the outer conductor alone or on both coaxial conductors, the latter being typical of VHF coaxial transmission lines [6, 7]. For example, Alcator C-Mod utilizes 10 cm, 50Ω copper coaxial transmission lines in vacuum for the Ion Cyclotron Radio Frequency heating (ICRF) systems [8]. ICRF systems commonly have short coaxial or stripline vacuum regions in transition from the pressurized line to the antenna located in vacuum. These short sections of vacuum transmission line are susceptible to multipactor and consequently low pressure glow discharges at neutral pressures below the Paschen breakdown value [4].

The Coaxial Multipactor Experiment (CMX) is designed to investigate multipactor discharges in both parallel plate and coaxial geometries. In both cases, CMX provides the first detailed electron distribution functions for various frequencies, geometries, and electrode materials. Section II describes the rf circuit in detail, and section III describes the multipactor current measurement and extraction of the distribution functions. Section IV describes the experimental procedure and results from both coaxial and parallel plate geometries.

II. RF EXPERIMENTAL SETUP

CMX produces a multipactor discharge in a 25.4 cm, stainless steel (SS), six-way cross called the Multipactor Vacuum Chamber (MVC) capable of a base pressure of 5×10^{-8} torr. Fig. 1 depicts both the coaxial and the parallel plate multipactor configurations. In each case, the vacuum region is given by the shaded area. The MVC uses a manual gas bleed valve to introduce a variety of gases at different pressures. The transmission line vacuum windows are Myat 401-050 gas barriers with Viton o-rings and Teflon barrier.

CMX investigates multipactor discharges in the frequency range of 40-150 MHz with RF power up to 1 kW in the high Q resonator (typical 1500, coaxial; 500, parallel plate). Because of the high Q of the cavity, voltages of order 1 kV can be achieved in the unmatched loop with a relatively low input power. A tuning network, consisting of a stub tuner and phase shifter pair, minimizes the reflected power to the source. RF power measurements include three pairs of directional couplers: one on the matched side, and a pair on each side of the vacuum chamber. In the parallel plate case, the last coupler pair is absent.

In the coaxial case, two vacuum windows allow the 50Ω, 10 cm outer diameter, copper transmission line to pass continuously through a 15 cm long vacuum section. This short length allows for minimum voltage variation along the vacuum section for the VHF frequencies of interest. By varying the length of an adjustable shorted stub at the end of the resonator, the maximum voltage of the standing wave pattern can be placed in the MVC. The multipactor discharge occurs in this coaxial region of the MVC. Both inner and outer conductors are cleaned for ultra high vacuum with no additional surface preparations; therefore, the coaxial conductors are placed into vacuum with a copper oxide layer.

In the parallel plate case, the center conductor of the gas barrier is extended into the center of the MVC. One multipactor electrode is attached to this center conductor, and the other electrode is grounded to the MVC by an aluminum ground strap. Teflon spacers prevent coaxial multipactoring in the short coaxial region of the gas break. The electrodes are 10 cm in diameter with separation ranging from 1 cm to 10 cm. Stainless steel, copper (oxidized and etched), and titanium (oxidized and etched) have been investigated thus far in parallel plate experiments. These metals were chosen because of their common use in rf system and their varied secondary emission coefficients. With the exception of pure titanium, all the electrode materials have a secondary emission coefficient $\delta(E) \geq 1$ at the multipactor electron energy [9, 10, 12]. The electrodes are typically vacuum conditioned by both multipactor and RF glow discharge. The oxide surfaces of both the copper and titanium electrodes can be removed by means of argon RF discharge etching.

In both coaxial and parallel plate configurations, the rf circuit is modeled by CST Microwave Studio in order to determine the voltage pattern inside the MVC from the circulating power measurement. Simulation results are found to be consistent with the directional couplers and the measured electron energy distributions. Examples of these distribution functions are discussed in section IV.

All rf signals are converted to DC signals by rf diodes, and each signal is digitized by a National Instruments 6071e digitizer. The signals are then recorded by the Matlab Data Acquisition Toolbox package.

III. MULTIPACTOR CURRENT MEASUREMENT

The multipactor electron currents and energy distributions are measured with retarding potential analyzers (RPAs). The same gridded analyzers are used in both coaxial and parallel plate configurations. Fig. 2 illustrates the analyzer geometry. The RPAs consist of a grounded entrance grid, a bias grid, and a collector plate. The three components are separated and electrically isolated by a 0.25 mm thick mica washer. The grid is made by spot-welding a 44% optical transmission, electroformed SS mesh to a 0.33 mm thick stainless steel washer. The RPA components are stacked inside a ceramic cylinder which is then mounted on the conductor of interest. A simple spring applies the necessary force to keep each component aligned and the entrance grid in good electrical contact with the conductor.

In the coaxial geometry, twelve RPAs are arranged azimuthally around the outer conductor, while in the parallel plate geometry, a single RPA is placed in the center of the grounded electrode. In all cases, the multipactor current enters through a 3.2 mm entrance aperture.

The bias grid is swept (0 to -500 V max) by a Kepco BOP 500M in order to collect the current as a function of bias voltage. In order to fully suppress any secondary emission, a minimum +20 V is maintained between the collector and bias grid by holding the collector fixed at +20 V while the bias grid voltage is swept negatively with a triangle waveform. The waveform is depicted in fig. 3.

A Keithley 6487 picoammeter measures the multipactor electron current from the collector. The picoammeter is held at the +20 V collector voltage relative to ground, and the ± 2 V analog output is then input to a simple differential amplifier to subtract the bias voltage, as shown in fig. 2. Careful attention was placed on stray capacitance and displacement current errors. A 15 pF capacitance between the collector and bias grid produces a displacement current as the bias grid voltage is swept. Fig. 3 illustrates the displacement current, which is proportional to ΔV and the capacitance. The 12 mV DC offset of the differential amplifier can also be seen in the figure. By holding the collector at fixed voltage and only sweeping the suppressor grid, the displacement current is minimized and can be averaged out using a smoothing spline function. Also, the suppressor grid is biased at a 1 Hz frequency to minimize the displacement currents. Examples of a CMX I-V characteristic and a electron distribution are shown in fig. 4. The distribution function is determined from the smoothed I-V characteristic by the method given by Hutchinson [11]. The details of the distribution functions at different geometries, frequencies, and surface conditions will be discussed in a future paper.

IV. EXPERIMENTAL OPERATION AND RESULTS

In order to initiate the multipactor discharge, the rf circuit is first tuned to the desired frequency with a network analyzer. The rf power is then manually increased in a stepwise manner, recording data at each power step as shown in the first panel of fig. 5. At multipactor onset, the reflection coefficient increases proportional to the multipactor current, as shown in the second and third panels of fig. 5. As the MVC voltage increases, the multipactor current increases until the multipactor pushes through the upper voltage limit, indicated as a drop in electron current and a jump in MVC voltage. Fig. 5 also depicts the electron distributions functions for each power step. The amount of power dissipated in the multipactor is determined from the distribution function. This power is typically $10 - 15\%$ of the input power, 8 to 10 W maximum.

Fig. 7 depicts the voltage onset of the multipactor discharge, which is often referred to as a susceptibility curve. The upper and lower voltage thresholds are calculated using the case of zero-energy electron emission model of Kishek [2]. CMX susceptibility data is shown for several electrode materials in the parallel plate configuration. Also shown is the parallel plate experimental data of R. Woo [13]. In general, CMX multipactor discharges typically occur between 100-400 V.

In all cases in both configurations, the distribution function has a sharp drop off at the MVC voltage, i.e. the maximium bulk electron energy is equal to the MVC voltage, as shown in fig. 6. This result indicates that the electron distribution data and MVC voltage measurement are consistent. Results are also consistent with the parallel plate, 50 MHz data of Hohn [4], and theoretical and experimental susceptibility data given in fig. 7.

Results from azimuthal measurements in the coaxial case show no azimuthal spatial variation of the multipactor. For the parallel plate geometry, no multipactor can be detected for pure titanium when the oxide layer is removed by argon etch.

V. SUMMARY

The Coaxial Multipactor Experiment provides a test-bed for studying multipactor discharges under various conditions in a parallel plate configuration and also extends the study of multipactoring to the coaxial geometry. The coaxial geometry is of interest in the fusion community because of the use of vacuum coaxial transmission lines for RF power. CMX produces multipactor discharges with a high Q resonant circuit and a high vacuum chamber. CMX allows detailed measurements of coaxial multipactor discharges and the electron distribution functions via retarding potential analyzers. With this information, a better understanding of coaxial multipactoring will lead to improved avoidance techniques and vacuum transmission line design.

[1] A.J. Hatch and H.B. Williams. *Phys. Rev.*, 112 (3), November 1958.

[2] R.A. Kishek et al. *Phys. Plasmas*, 5 (5), May 1998.

[3] J.M. Vaughan. *IEEE Trans. Electron Devices*, 35 (7), July 1998.

[4] F. Hohn et al. *Phys. Plasmas*, 4 (4), April 1997.

[5] E.W.B. Gill and A. von Engel. *Proc. R. Soc. London, Ser. A*, 192 (446), 1948.

[6] T.P. Graves et al. Experimental Results of the Coaxial Multipactor Experiment (CMX). In *16th Topical Conf. on Radio Frequency Power in Plasmas*, Park City, UT, 2005.

[7] R. Woo. *J. Appl. Phys.*, 39 (3), May 1968.

[8] Y. Takase et al. Engineering Design and Analysis of the Alcator C-Mod Two-strap ICRF Antenna. In *14th Symp. on Fusion Engineering*, San Diego, CA, 1992. IEEE.

[9] V. Baglin et al. The Secondary Electron Yield of Technical Materials and its Variation with Surface Treatments. In *7th European Particle Accelerator Conference*, Vienna, Austria, 2000.

[10] D.R. Lide. *Handbook of Chemistry and Physics, 72nd ed.*, CRC Press, 1991.

[11] I.H. Hutchinson. *Principles of Plasma Diagnostics.* Cambridge University Press, Cambridge, UK, 2002.

[12] D. Ruzic et al. *J. Vac. Sci. Technol.*, 20 (4), 1982.

[13] R. Woo. Final Report on RF Voltage Breakdown in Coaxial Transmission Lines. Technical Report 32-1500, NASA-JPL, 1970.

Caption Page

Fig. 1: CMX Experimental setup for both (a) coaxial and (b) parallel plate multipactor discharges.

Fig. 2: Schematic drawing of retarding potential analyzers used to determine electron current and distributions.

Fig. 3: CMX voltage and current signals for non-multipactor case.

Fig. 4: I-V characteristic for coaxial geometry, 60 MHz, 3.2 W multipactor, $V_{MVC} = 212V$.

Fig. 5: RF and multipactor electron current data for 70 MHz, coaxial geometry, copper outer conductor. The electron distributions at each MVC voltage are shown in the lower panel.

Fig. 6: Expanded view of high energy portion of the electron distributions functions in fig. 5 displayed as a contour plot.

Fig. 7: CMX Multipactor Susceptibility for parallel plates as compared to experimental and theoretical values [2, 13].

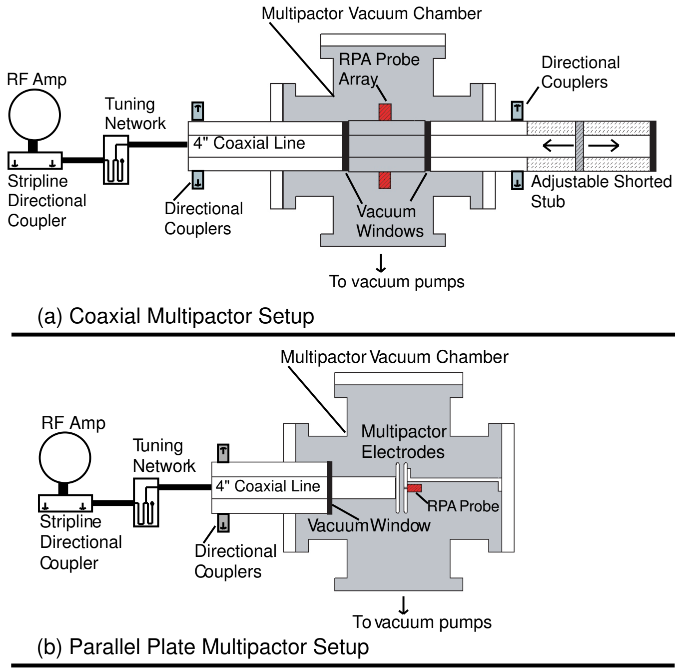

FIG. 1: CMX Experimental setup for both (a) coaxial and (b) parallel plate multipactor discharges.

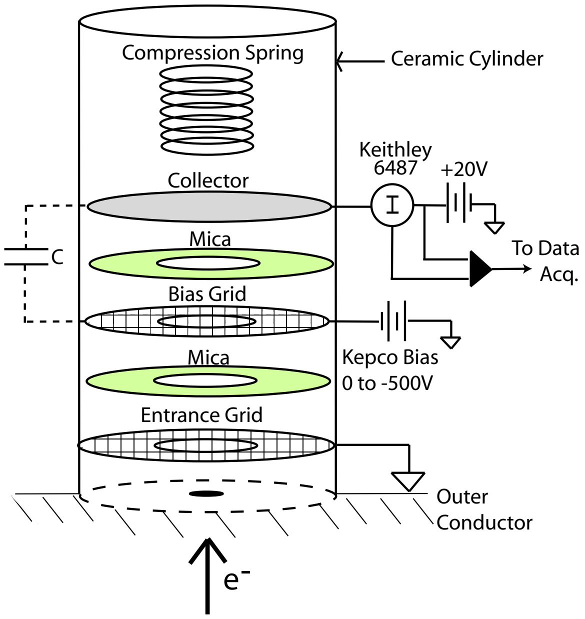

FIG. 2: Schematic drawing of retarding potential analyzers used to determine electron current and distributions.

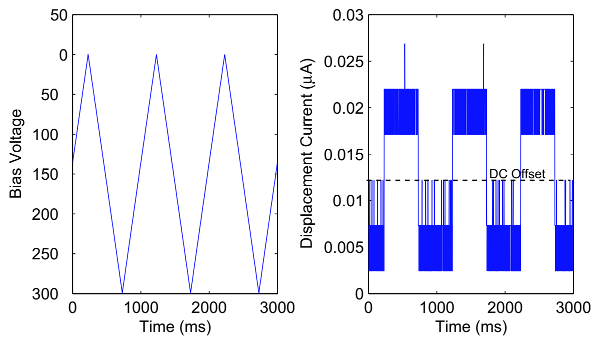

FIG. 3: CMX voltage and current signals for non-multipactor case.

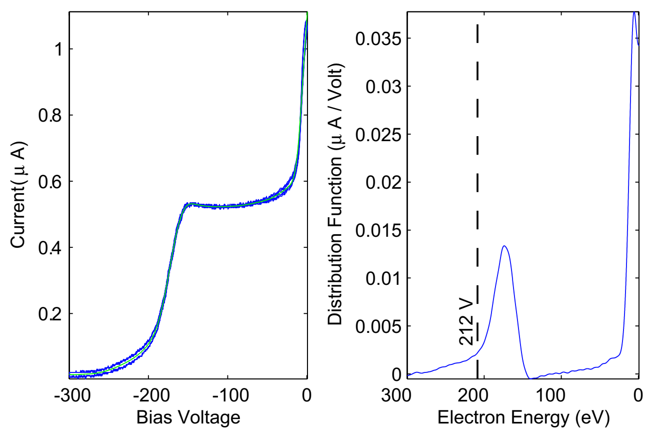

FIG. 4: I-V characteristic for coaxial geometry, 60 MHz, 3.2 W multipactor, $V_{MVC} = 212V$.

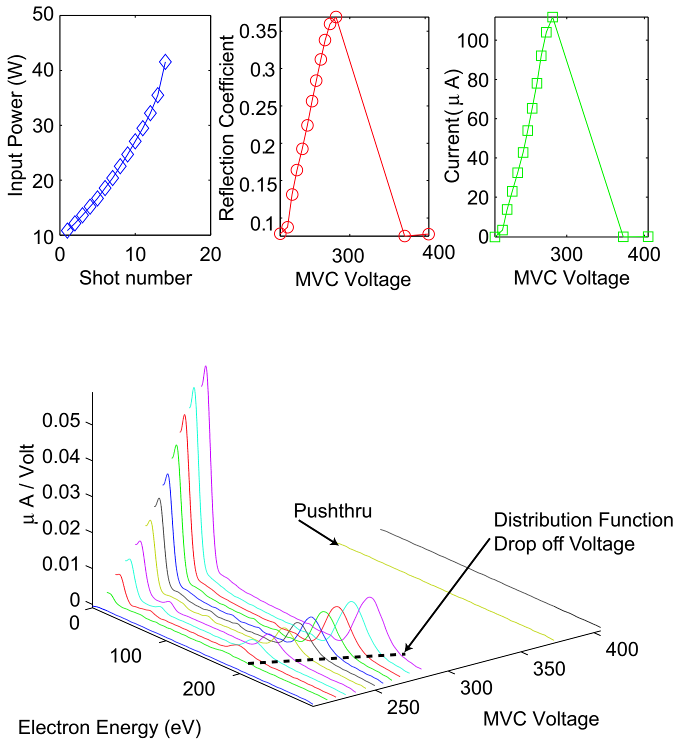

FIG. 5: RF and multipactor electron current data for 70 MHz, coaxial geometry, copper outer conductor. The electron distributions at each MVC voltage are shown in the lower panel.

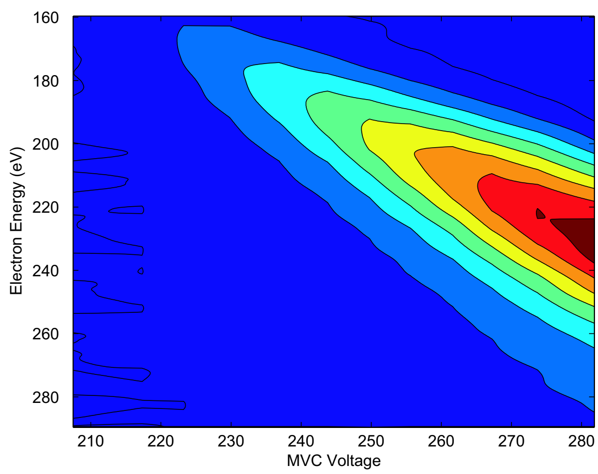

FIG. 6: Expanded view of high energy portion of the electron distributions functions in fig. 5 displayed as a contour plot.

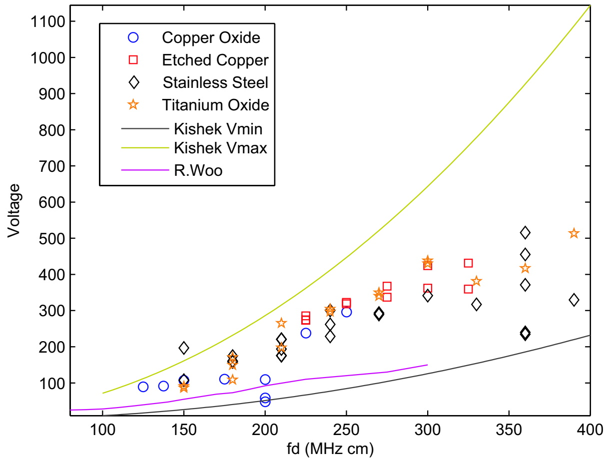

FIG. 7: CMX Multipactor Susceptibility for parallel plates as compared to experimental and theoretical values [2, 13].